High yield formation of lipid bilayer shells around silicon nanowires in aqueous solution

2013 Nanotechnology 24 355601

(http://iopscience.iop.org/0957-4484/24/35/355601)

Nanotechnology **24** (2013) 355601 (7pp) doi:10.1088/0957-4484/24/35/355601

High yield formation of lipid bilayer shells around silicon nanowires in aqueous solution

Lotta Römhildt[1,4], Andreas Gang[1,4], Larysa Baraban[1], Jörg Opitz[1,2] and Gianaurelio Cuniberti[1,3]

[1] Institute for Materials Science and Max Bergmann Center of Biomaterials, TU Dresden, 01062 Dresden, Germany
[2] Fraunhofer Institute IZFP, 01109 Dresden, Germany
[3] Division of IT Convergence Engineering, POSTECH, Pohang 790–784, Korea

E-mail: larysa.baraban@nano.tu-dresden.de

Received 28 March 2013, in final form 26 June 2013
Published 6 August 2013
Online at stacks.iop.org/Nano/24/355601

Abstract
The combination of nanoscaled materials and biological self-assembly is a key step for the development of novel approaches for biotechnology and bionanoelectronic devices. Here we propose a route to merge these two subsystems and report on the formation of highly concentrated aqueous solutions of silanized silicon nanowires wrapped in a lipid bilayer shell. We developed protocols and investigated the dynamics of lipid films on both planar surfaces and silicon nanowires using fluorescence recovery after photobleaching, demonstrating fully intact and fluid bilayers without the presence of a lipid molecule reservoir. Finally, the experimental setup allowed for *in situ* observation of spontaneous bilayer formation around the nanowire by lipid diffusion from a vesicle to the nanowire. Such aqueous solutions of lipid coated nanowires are a versatile tool for characterization purposes and are relevant for newly emerging bioinspired electronics and nanosensorics.

S Online supplementary data available from stacks.iop.org/Nano/24/355601/mmedia

(Some figures may appear in colour only in the online journal)

1. Introduction

Bringing together biological molecules with inorganic nanosized materials offers enhanced functionalities of existing nanoscale devices. Investigations of silicon nanowires (SiNWs) currently attract a great deal of attention [1, 2]. A key reason for this is that nanowires reside at the frontier between nanoresearch and biotechnology related studies [3, 4]. On one hand, nanowire based concepts are considered as a novel paradigm for the development of future electronic devices [5, 6]. On the other hand, nanowires by themselves can represent an ultrasensitive platform for real time and label-free biosensing when integrated in field effect transistor devices (FETs) [7–9].

Lipid bilayers as biological materials have already been used to functionalize surfaces for biosensing, e.g. in quartz crystal microbalance measurements [10], on metal oxide semiconductor FETs [11] or SiNW based FETs [12]. With the incorporation of membrane proteins that form pores with regard to chemical changes in the surrounding media, biological processes like enzymatic reactions can be monitored [12]. Lipid bilayer coating of nanowires could also be important to provide biocompatible surfaces when electrical characteristics of single cells are measured using kinked nanowires [13–15].

Bilayers have potential to mimic cell membranes in the study of transportation mechanisms through membrane channels or drug influences on the membrane stability [16]. Furthermore, lipids can enhance the biocompatibility of small particles for medical purposes such as drug delivery [17–19].

[4] These authors contributed equally to this work.

The degree of membrane curvature plays an important role for membrane proteins in cells. Curvature changes might influence certain intracellular processes governed by the transport properties of the membrane [20]. Therefore the coating of curved small objects such as carbon nanotubes (CNTs) [21] or nanowires [22] is also of fundamental interest [23].

One-dimensional (1D) structures of lipid bilayers have been reported by Kulkarni *et al* [24] using specially designed combinations of lipids that form cylindrical tube-like structures without the support of a template. The group of Noy *et al* [21] presented a protocol to completely wrap polymer coated CNTs dispersed on a TEM grid with a functional lipid bilayer. A similar protocol was applied to polysilicon nanowires which were also dispersed on a TEM grid before lipid bilayer coating [22]. However, bottom-up ways of integration of nanowires or nanotubes into devices are still a challenge [25, 26]. The combination of the self-assembly properties of biological material together with nanoparticles can lead to controlled deposition of these nanoparticles [27], *e.g.* on bacterial S-layer templates [28].

Despite a large number of reports on the formation of lipid bilayer coatings and even their interactions with silicon nanowires, the formation of highly concentrated aqueous solutions containing suspended nanowires wrapped by lipid films has not been demonstrated so far. At the same time it should be stressed that solutions containing such functional nanowires are of special interest for the wide range of biotechnological applications, from drug delivery purposes to multiparallel sensor arrays.

Here we present a reproducible strategy on how to obtain SiNWs dispersed in an aqueous solution as carriers of one-dimensional lipid bilayers, by combining a suspension stabilizing surface functionalization of the SiNWs as suggested by Heo *et al* [25] with a common lipid bilayer deposition approach. We firstly demonstrate the applicability of our lipid bilayer formation parameters on planar surfaces (see figure 1(A)). Then we show the transfer of the protocol onto the curved surface of SiNWs (see figure 1(B)). The optimal pH range was determined via zeta-potential measurements. Dynamics of the lipid films were investigated using the fluorescence recovery after photobleaching (FRAP) technique. *In situ* observations of lipid exchanges between a vesicle and the bilayer coating of a SiNW demonstrate that SiNWs are suitable templates. The obtained 1D lipid bilayer structures could be used as drug delivery agents or they might be integrated into devices as actuator elements in bionanosensors based on SiNWs.

2. Materials and methods

2.1. Preparation of vesicle solutions

In order to form vesicles, DOPC lipids (glycophospholipid 1,2-dioleoyl-sn-glycero-3-phosphocholine) were employed. 2 mol% of headgroup-labelled NBD-PE lipids (1,2-dioleoyl-sn-glycero-3-phosphoethanolamine-N-7-nitro-2- 1,3-benzoxadiazol-4-yl, both lipids from Avanti Polar Lipids, Inc.) were added to stain vesicles with fluorophores for optical detection. Unilamellar vesicle (ULV) solutions were prepared from stock solutions of 1 mg ml^{-1} (DOPC) and 0.1 mg ml^{-1} (NBD-PE) lipids in chloroform. Required amounts were transferred into a flask and dried via nitrogen flow and subsequent vacuum pumping. The resulting thin film of dried lipids was dispersed in the chosen buffer. The blurry solution was left for strong sonication until the solution clarified, indicating the formation of unilamellar vesicles. ULVs can be further used to create lipid bilayers on a solid support. Different buffers (sodium acetate, MES and TRIS) with pH values ranging from 5.0 to 8.1 were tested for the bilayer formation and 12 mM sodium acetate buffer (chemicals from Sigma Aldrich Co. LLC) at pH 5.0 led to the desired functional lipid bilayers on APTES-functionalized surfaces. Other systems resulted in bilayer formation as well, but they were less homogeneous, with patches and a slower recovery in FRAP (data not shown here).

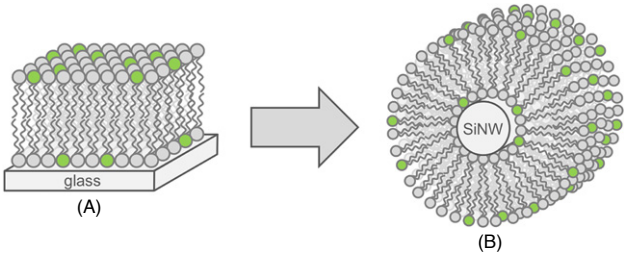

Figure 1. Testing on planar substrates and protocol transfer to silicon nanowire.

2.2. Substrate preparation

Firstly, we focused on investigating bilayer formation parameters and improving bilayer qualities on planar and functionalized glass substrates. After cleaning in acetone and isopropanol, the slides were dried under nitrogen gas flow. Hydroxyl groups were activated using oxygen plasma for 20 s to enable attachment of 3-aminopropyltriethoxysilane (APTES, Sigma Aldrich). Before substrate immersion, the 2 vol-% APTES solution in an absolute ethanol and dd-H_2O mixture (95:5, v/v) was left for 10 min to hydrolyse. The activated slides were then incubated for 2 min, rinsed successively in two ethanol baths and one dd-H_2O bath, dried under N_2 flow and postbaked at 120 °C for 10 min. For supported lipid bilayer (SLB) formation, droplets of the vesicle solutions were suspended on APTES-functionalized glass cover slides. After addition of calcium chloride with Ca^{+2} concentrations up to 50 mM, the allowed SLB formation time was at least 1 h, followed by buffer rinsing to remove loose vesicles from the surface. The bilayer thickness in the buffer was measured with an ellipsometer in a liquid cell setup (Sentech ellipsometer) and could be determined to be in the range of 4–5 nm with a refractive index of 1.45 [29]. This is in good agreement with previously reported values for DOPC lipids [30]. The same protocol was later applied to the nanowire solutions.

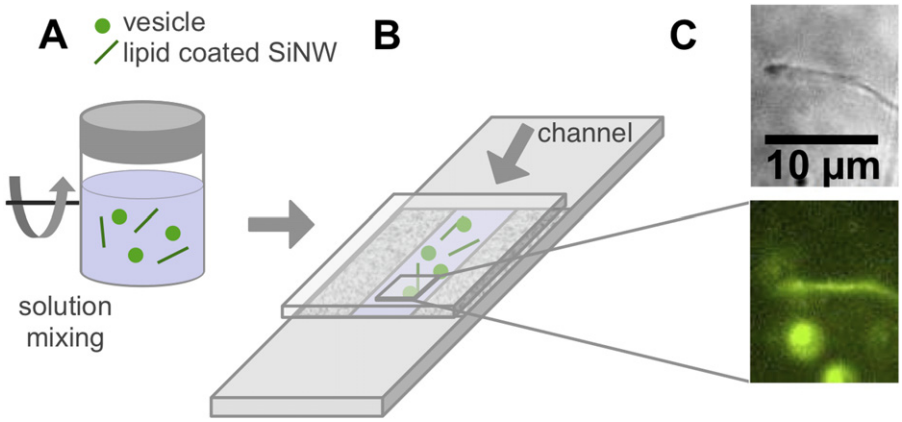

Figure 2. (A) Schematic procedure of vesicle–nanowire mixing, and (B) channel setup for microscopy of nanowire and vesicle solutions. (C) The same nanowire is shown with optical and fluorescence microscopy. With fluorescence also vesicles are visible.

SiNWs as the substrate material were grown by means of the vapour–liquid–solid method [26, 31] using gold nanoparticles as catalysts [2]. The length of the wires was in the range of 1–10 μm, the average diameter 20 nm. For the purposes of various experiments, bottom-up grown SiNWs have to be detached from the growth substrate and redispersed in liquid media. Usually, the substrates are sonicated in organic solvents where the SiNWs do not agglomerate with time [22, 2]. In order to create a bilayer shell around the nanowire, however, use of an aqueous solution is necessary. Once the NW suspension is mixed with the vesicle solution (see figure 2(A)), vesicles adsorb onto the surface. Lipid bilayers are formed around the nanowires by fusion and rupture of unilamellar vesicles following the different mechanisms proposed by Richter *et al* [32]. The nanowire represents the substrate for SLB formation.

Heo *et al* [25] demonstrated that SiNWs functionalized with APTES remain stable in ddH_2O by electrostatic repulsion due to the protonation of the primary amine surface group. NW solutions were prepared following their protocol. The wafers with grown SiNWs were cleaned for 20 s in oxygen plasma and immediately covered with the APTES solution. After 20 min of incubation, growth substrates were immersed in three subsequent ethanol baths and postbaked at 120 °C for 5 min. The functionalized growth substrates were sonicated in ddH_2O for 2 min to create aqueous nanowire dispersion. After successful surface modification the solution appears yellowish indicating well dispersed nanowires. In order to determine the efficiency of surface functionalization, the zeta potential (ζ) of nanowires dispersed in the solution was measured (Zetasizer nano ZS, Malvern Instruments Ltd/Malvern/GB). As illustrated in figure 3, APTES-SiNWs have ζ-potential values of 19–22 mV at pH 5.8–6.0 (measured pH of ddH_2O). According to Wu *et al* [33], silica particles with APTES coating show an isoelectric point at approximately pH 9, whereas at pH 5 the ζ-potential is 20–22 mV. The nanowire characteristics are thus in perfect agreement with the data from Wu *et al* [33] for the selected pH range (see grey bar in figure 3), also indicating the successful surface modification with APTES. The determined isoelectric point for APTES coated SiNWs

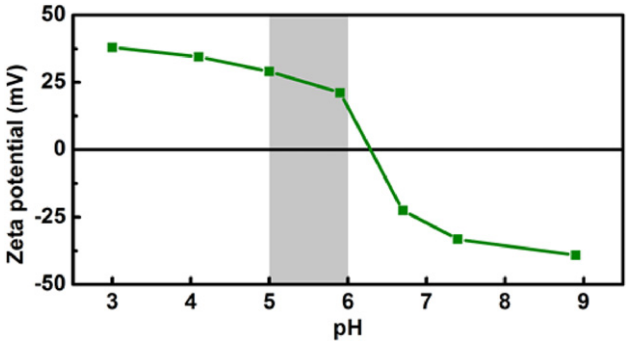

Figure 3. Zeta potential of APTES coated SiNWs in ddH_2O, measured from pH 3 to 9. The grey bar highlights the pH region spanned by both solutions used: ddH_2O for zeta potential and acetate buffer for bilayer wrapping experiments.

with 6.5 is however lower. The discrepancy might be due to the high aspect ratio of nanowires not corresponding to the fully spherical model assumed in ζ-potential calculation. In addition, the APTES density might influence the shift. By measuring the zeta potential and characterizing the bilayer quality at different pH values we optimized the conditions for SLB formation around NWs (grey area in figure 3). Crossing the isoelectric points towards higher pH value leads to deprotonation of the amines whereas lower pH results in less homogeneous bilayer shells.

2.3. Fluorescence recovery after photobleaching

Formation of SLBs was investigated using a fluorescence recovery after photobleaching (FRAP) technique. Here, a Zeiss Axiovert 200M microscope in combination with a Photometrics Cascade 512B camera and Zeiss filterset 09 were utilized. The NBD-labelled films were locally photobleached at minimally opened aperture resulting in dark spots of diameters of approximately 18 μm. After bleaching, the aperture was opened manually and an image recording series of this area was started (first image 1 sec after bleaching; MetaVue imaging software, maximum two images per second). The recovery of the fluorescence in the bilayer

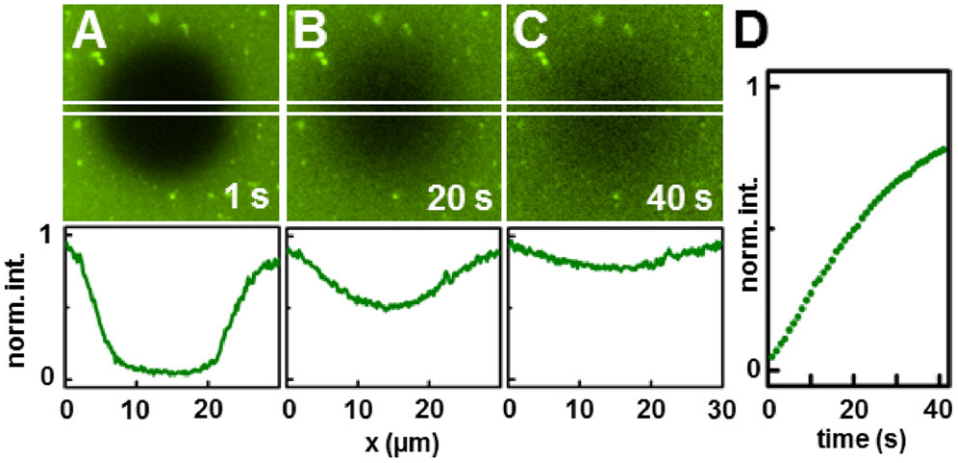

Figure 4. Result of a FRAP experiment performed on an SLB deposited on an APTES-functionalized glass cover slide from an acetate buffered (12 mM, pH 5) vesicle solution. Fluorescence images and the according normalized fluorescence intensity profiles along the stripe within the two white lines over the bleached spot after (A) 1 s, (B) 20 s and (C) 40 s. (D) The time dependent recovery of the fluorescence intensity in the middle of the bleached spot—approx. 75% fluorescence intensity compared with the initial state recovered after 40 s.

was evaluated by analysing the grey values of the recorded images. A high grey value is assumed to be equivalent to a high degree of fluorescence.

The vesicle–nanowire solutions were monitored in a fluid channel setup as presented in figure 2(B). Two stripes of double-sided adhesive tape on a microscope glass slide leave a thin channel. A glass cover slide is glued on top to close the channel. Due to capillary forces, sample solutions positioned at the channel openings using a pipette are sucked in and can be monitored readily. As a consequence of the confined space focusing of moving objects such as vesicles or nanowires is facilitated.

3. Results and discussion

3.1. Lipid bilayers on planar surfaces

In figure 4 fluorescence microscopy images of a bilayer formed on an APTES-functionalized glass cover slide within an acetate buffer solution are presented. The dark spot in the middle of the images results from a photobleaching procedure as described above (see section 2.3). The fluorescence recovery after bleaching the circular area at 1, 20 and 40 s (see corresponding images in figures 4(A)–(C)) is depicted. Below the fluorescence images, the respective normalized fluorescence intensities along the stripes between the two white lines are plotted. In figure 4(D), the time dependence of the fluorescence recovery at $x = 15.5\ \mu\text{m} \pm 1.5\ \mu\text{m}$ (minimum position) is shown. At 40 s approximately 75% of the initial fluorescence is recovered. After fast recovery in the first seconds, the intensity approaches a saturation level below the original intensity level. This saturation level depends on the bilayer quality. Our results indicate that under the chosen conditions intact SLBs, with a few vesicles attached on top, are formed. Further improvement might be necessary to fulfil the need for defect-free bilayers in electronic applications [34]. In good approximation, the intensity profile directly after bleaching ($t = 0$) is of rectangular shape with a width of $d = 2 \cdot w = 18\,\mu\text{m}$ which allows estimation of a diffusion coefficient D after Soumpasis [35]. At $t_{1/2} = 20$ s, 50% of the original intensity level is reached and D can be calculated as follows:

$$D = 0.224 \cdot w^2/t_{1/2} = 0.9\,\mu\text{m}^2\ \text{s}^{-1}. \quad (1)$$

The determined diffusion coefficient is slightly lower than the previously reported values of 2–10 $\mu\text{m}^2\ \text{s}^{-1}$ for lipid diffusion on more hydrophilic substrates [36]. This discrepancy can be explained by the lower hydrophilicity of our samples. The contact angle of water on APTES-functionalized SiO_2 surfaces was measured to be between $45° \pm 5.0°$ for glass and $60.1° \pm 6.0°$ for Si wafers with native oxide, compared to values below 10° for blank glass and wafer samples. Hydrophobic substrates with contact angles above 90° may hinder bilayer formation on nano-objects [37] which might lead to a further decrease of the diffusion coefficient of the molecules and prevent bilayer formation. In contrast, the charge of protonated amines present in APTES may promote DOPC lipid bilayer formation, as Leonenko *et al* investigated for APTES-modified mica [38] and lipid bilayers successfully formed on top of amine terminated CNTs integrated in FETs [39]. Thus, we conclude that we have stable and homogeneous bilayers with lowered lipid mobility because of electrostatic interactions due to the surface modification.

3.2. Lipid bilayers around SiNWs

In order to coat the nanowires dispersed in water with a lipid bilayer shell, vesicle solutions consisting of ULVs were mixed with the APTES coated SiNW solution at a 1:1 ratio (v/v). The SiNW–vesicle solution was constantly mixed together with Ca^{+2} ions for 1 h (see figure 2(A)). This solution was observed in the as-mixed state using a setup as shown in figure 2(B). Figure 2(C) shows two images taken successively at one position of a SiNW–vesicle solution

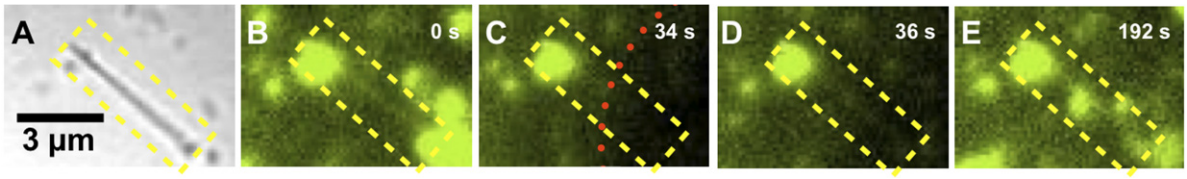

Figure 5. Series of optical and fluorescence microscopy images from $t = 0$ s (A) to 280 s (B), showing vesicles and a bilayer coated nanowire which is indicated by the dashed line frame. An area partially including the nanowire is photobleached (area right of the dotted line) (C). Fast recovery of the bilayer fluorescence on the bleached part of the nanowire in 2 s from image (C) to (D) is observable. In image (E) the spot including the wire surface appears fully recovered.

mixture. In brightfield settings (upper image) a SiNW can be observed. Although having a diameter of only around 20 nm the NW is discernable as it diffracts the light. This is also well above the critical diameter for lipid membrane curvature of 5 nm, as reported elsewhere [40]. Thus, no further thickness increase of the 1D template is required, compared to *e.g.* thinner single-walled CNTs [21, 41]. Due to Brownian motion the NW moves inside its fluid environment variantly leaving and entering the focus plane (see movie 1 in ESI available at stacks.iop.org/Nano/24/355601/mmedia). The same SiNW can be observed in the fluorescent light image (see figure 2(C), lower image) next to vesicles floating in the solution. As the focus plane is in the middle of the channel and not on the glass cover slide, possible vesicles and bilayers which are out of focus result only in a low background fluorescence. This makes the NW clearly distinguishable from its surroundings. The fluorescence is homogeneous along the whole NW and thus it is fully coated by a lipid shell. Statistical evaluation of 82 nanowires was carried out. 26% of the NWs could not be evaluated, as the fluorescence of a possible coating was overshone by attached vesicles. 54% of the NWs were covered in a bilayer shell and the remaining 20% did not show a fluorescence signal. Longer incubation times will probably increase the chances for SLB formation on uncoated NWs. According to Dayani *et al* [41], 1D templates of comparable diameter with a lipid bilayer shell are stable in buffer solution for 60 days. Moura *et al* [42] reported single stabilization of a colloidal solution of lipid coated silica particles when intact single bilayers cover the surface with a saturated phosphocholine density. We conclude that SiNWs coated with functional lipid bilayers are also stable in the buffer solution due to steric stabilization by the thin lipid shell.

Functional lipid bilayers are defined by the ability of the lipid molecules to diffuse within the layer and heal defects [21]. In figure 5, a FRAP experiment involving parts of a nanowire is shown (nanowire indicated within the dashed line frame). Along the wire an increased fluorescence brightness is observable (figure 5(B)). After photobleaching of part of the area, indicated by the dotted line in figure 5(C), the fluorescence along the wire has disappeared. We conclude that this confirms that the glow along the wires is not a consequence of *e.g.* scattering the fluorescent light of surrounding sources but results from the bilayer itself.

Two seconds after photobleaching (see figure 5(D)), the majority of fluorescence on the nanowire has already recovered, indicated by a reincrease in intensity, whereas the remaining area of the bleaching spot still appears dark. This could mean that the diffusion coefficient on the wire is higher than on the flat substrate underneath. This is consistent with bilayers on 55 nm diameter nanowires investigated by Huang *et al* [22] who studied the influence of the substrate curvature on the bilayer dynamics and found higher recovery velocities than on planar substrates. After 3 min, the fluorescence along the wire as well as within the rest of the bleached spot has reached its original fluorescence intensity (see figure 5(E)) .

Figure 6 displays a time series of optical and fluorescent images observing the interaction of a vesicle with an APTES-NW *in situ* (see also movie 2 in ESI available at stacks.iop.org/Nano/24/355601/mmedia). The vesicle is moving due to Brownian motion and approaches the wire at $t = 62$ s (indicated by an arrow in figure 6(B)). Within the following 22 s the vesicle attaches to the wire via physisorption and detaches again (indicated by an arrow in figure 6(C)). As a consequence of the contact, a fluorescence intensity increase at the tip of the nanowire is observable compared to $t = 0$ s. We assume that lipid molecules were transferred from the attached vesicle into the already existing bilayer at the SiNW tip during the contact time. Most probably, the fluorescence intensity increase around the nanowire occurred due to these additional NBD-PE lipids. Furthermore, it is possible that the sharp tip of the nanowire mechanically pulls out parts of the vesicle membrane, also resulting in a transfer of lipids from the vesicle to the nanowire that acts as a template for SLB formation.

4. Conclusions

Here we demonstrate highly concentrated aqueous solutions of silicon nanowires wrapped in a lipid shell. We optimized the conditions for lipid bilayer formation by characterizing the surface charge of these functionalized NWs using ζ-potential measurements. The rapid fluorescence recovery on the nanowires indicated functional lipid bilayers with high lipid mobility, which is crucial for stable solutions. With the presented channel setup, dynamic processes can also be studied *in situ* as exemplarily shown in figure 6.

The semiconducting and highly sensitive characteristics of SiNWs make them an interesting nanomaterial for research and other applications. Device integration for nanoelectronics is important for technological purposes such as biosensorics. For the development of bottom-up processes in contrast to

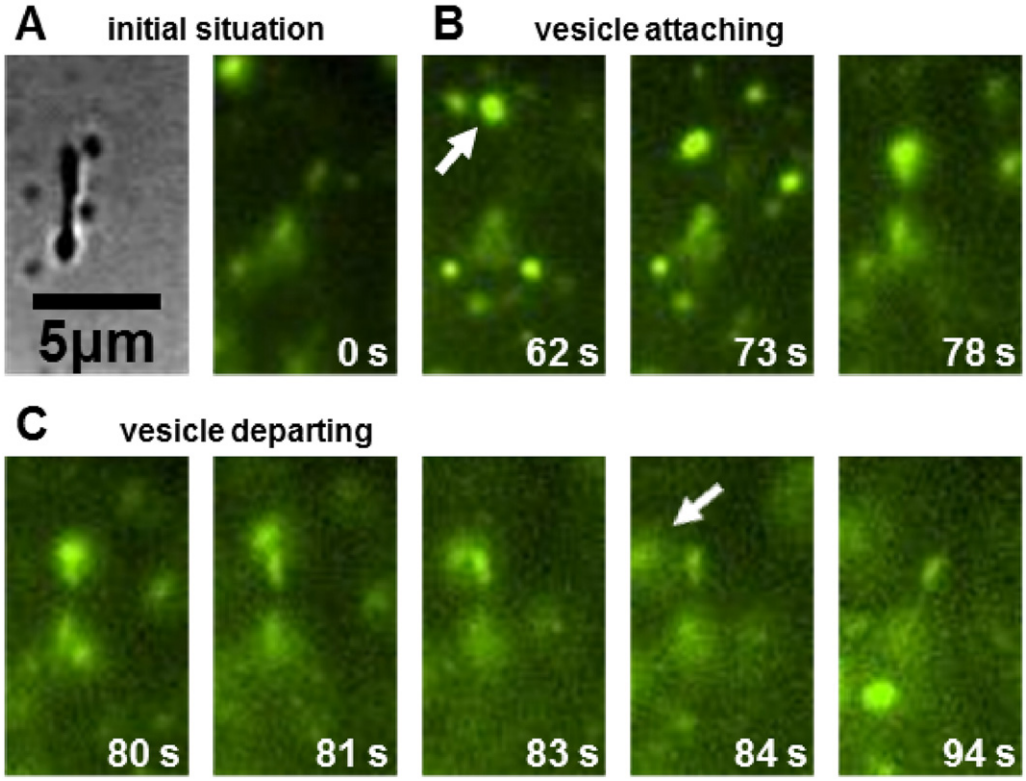

Figure 6. *In situ* observation of a ULV approaching an APTES–SiNW and leaving it (indicated by arrows). (A) Initial situation and nanowire position. (B) Vesicle arrives and attaches to the wire surface. (C) During contact time, lipid molecules from the vesicle diffuse onto the nanowire before the vesicle detaches again. The time range is from 0 to 94 s.

conventional top-down technologies, biological self-assembly can be used as a positioning tool. In this case, our developed method of highly concentrated lipid coated SiNWs in aqueous solution can be used together with the incorporation of functional lipid molecules such as biotinylated lipids. In combination with the strong biorecognition between biotin and streptavidin, this can be one option for creating SiNW arrays. In addition, knowledge regarding functional lipid bilayers on small curved objects helps to integrate lipid films as non-covalent functionalization layers in *e.g.* NW based FETs preventing the issue of unspecific protein adsorption. The advantage of bilayer coating in solution over techniques on substrates like TEM grids is that NW–lipid structures within the solution can be easily studied with a variety of techniques such as UV/Vis spectroscopy or, suspended onto different substrates, with TEM or AFM.

Acknowledgments

LR and AG gratefully acknowledge the supply of NW growth substrates from S Pregl and Namlab GmbH. LR and LB would like to thank A Caspari from IPF Dresden for kind cooperation with ζ-potential measurements. This work is funded by the European Union (ERDF) and the Free State of Saxony via the ESF project 080942409 InnovaSens. We gratefully acknowledge support from the German Excellence Initiative via the Cluster of Excellence EXC 1056 Center for Advancing Electronics Dresden (cfAED).

References

[1] Cui Y, Duan X, Hu J and Lieber C M 2000 Doping and electrical transport in silicon nanowires *J. Phys. Chem.* B **104** 5214–6

[2] Weber W M, Geelhaar L, Graham A P, Unger E, Duesberg G S, Liebau M, Pamler W, Cheze C, Riechert H and Lugli P 2006 Silicon-nanowire transistors with intruded nickel-silicide contacts *Nano Lett.* **6** 2660–6

[3] Park T J, Lee S J, Park J P, Yang M H, Choi J H and Lee S Y 2011 Characterization of a bacterial self-assembly surface layer protein and its application as an electrical nanobiosensor *J. Nanosci. Nanotechnol.* **11** 402–7

[4] Dawood M K, Zhou L, Zheng H, Cheng H, Wan G, Rajagopalan R, Too H P and Choi W K 2012 Nanostructured si-nanowire microarrays for enhanced-performance bio-analytics *Lab. Chip* **12** 5016–24

[5] Pregl S, Weber W M, Nozaki D, Kunstmann J, Baraban L, Opitz J, Mikolajick T and Cuniberti G 2013 Parallel arrays of Schottky barrier nanowire field effect transistors: nanoscopic effects for macroscopic current output *Nano Res.* **6** 381–8

[6] Sciacca C and Herfurth N 2011 Press release: IBM research—zurich uses nanowires to build transistors of the future www.zurich.ibm.com/pdf/nanocenter/Nanowires_en.pdf

[7] Cui Y, Wei Q, Park H and Lieber C M 2001 Nanowire nanosensors for highly sensitive and selective detection of biological and chemical species *Science* **293** 1289

[8] Kim K S, Lee H S, Yang J A, Jo M H and Hahn S K 2009 The fabrication, characterization and application of aptamer-functionalized Si-nanowire FET biosensors *Nanotechnology* **20** 235501

[9] GhoshMoulick R, Vu X T, Gilles S, Mayer D, Offenhaeusser A and Ingebrandt S 2009 Impedimetric detection of covalently attached biomolecules on field-effect transistors *Phys. Status Solidi* a **206** 417–25

[10] Höök F, Ray A, Norden B and Kasemo B 2001 Characterization of PNA and DNA immobilization and subsequent hybridization with DNA using acoustic-shear-wave attenuation measurements *Langmuir* **17** 8305–12

[11] Bavli D, Tkachev M, Piwonski H, Capua E, deAlbuquerque I, Bensimon D, Haran G and Naaman R 2012 Detection and quantification through a lipid membrane using the molecularly controlled semiconductor resistor *Langmuir* **28** 1020–8

[12] Misra N, Martinez J A, Huang S C J, Wang Y, Stroeve P, Grigoropoulos C P and Noy A 2009 Bioelectronic silicon nanowire devices using functional membrane proteins *Proc. Natl Acad. Sci.* **106** 13780

[13] Tian B, Cohen-Karni T i, Qing Q, Duan X, Xie P and Lieber C M 2010 Three-dimensional, flexible nanoscale field-effect transistors as localized bioprobes *Science* **329** 830–4

[14] Jiang Z, Qing Q, Xie P, Gao R and Lieber C M 2012 Kinked pn junction nanowire probes for high spatial resolution sensing and intracellular recording *Nano Lett.* **12** 1711–6

[15] Duan X, Gao R, Xie P, Cohen-Karni T, Qing Q, Choe H S, Tian B, Jiang X and Lieber C M 2012 Intracellular recordings of action potentials by an extracellular nanoscale field-effect transistor *Nature Nanotechnol.* **7** 174–9

[16] Petrak V, Grieten L, Taylor A, Fendrych F, Ledvina M, Janssens S D, Nesladek M, Haenen K and Wagner P 2011 Monitoring of peptide induced disruption of artificial lipid membrane constructed on boron-doped nanocrystalline diamond by electrochemical impedance spectroscopy *Phys. Status Solidi* a **208** 2099–103

[17] Liu J, Jiang X, Ashley C and Brinker C J 2009 Electrostatically mediated liposome fusion and lipid exchange with a nanoparticle-supported bilayer for control of surface charge, drug containment, and delivery *J. Am. Chem. Soc.* **131** 7567–9

[18] Ashley C E *et al* 2011 The targeted delivery of multicomponent cargos to cancer cells by nanoporous particle-supported lipid bilayers *Nature Mater.* **10** 389–97

[19] Goutayer M, Dufort S, Josserand V, Royère A, Heinrich E, Vinet F, Bibette J, Coll J-L and Texier I 2010 Tumor targeting of functionalized lipid nanoparticles: assessment by *in vivo* fluorescence imaging *Eur. J. Pharm. Biopharm.* **75** 137–47

[20] Zhou X, Moran-Mirabel J M, Craighead H G and McEuen P L 2007 Supported lipid bilayer/carbon nanotube hybrids *Nature Nanotechnol.* **2** 185–90

[21] Artyukhin A B, Shestakov A, Harper J, Bakajin O, Stroeve P and Noy A 2005 Functional one-dimensional lipid bilayers on carbon nanotube templates *J. Am. Chem. Soc.* **127** 7538–42

[22] Huang S, Artyukhin A, Martinez J and Sirbuly D 2007 Formation, stability, and mobility of one-dimensional lipid bilayers on polysilicon nanowires *Nano Lett.* **7** 3355–9

[23] McMahon H T and Gallop J L 2005 Membrane curvature and mechanisms of dynamic cell membrane remodelling *Nature* **438** 590–6

[24] Kulkarni V S, Anderson W H and Brown R E 1995 Bilayer nanotubes and helical ribbons formed by hydrated galactosylceramides: acyl chain and headgroup effects *Biophys. J.* **69** 1976–86

[25] Heo K, Cho E, Yang J E, Kim M H, Lee M, Lee B Y, Kwon S G, Lee M S, Jo M H and Choi H J 2008 Large-scale assembly of silicon nanowire network-based devices using conventional microfabrication facilities *Nano Lett.* **8** 4523–7

[26] Pregl S, Römhildt L, Weber W M, Baraban L, Opitz J, Mikolajik T and Cuniberti G 2012 Investigations on the sensing mechanisms in silicon nanowire schottky-barrier field effect sensors *Proc. IMCS 2012—14th Int. Meeting on Chemical Sensors;* pp 994–9

[27] Kinge S, Crego-Calama M and Reinhoudt D 2008 Self-assembling nanoparticles at surfaces and interfaces *ChemPhysChem* **9** 20–42

[28] Queitsch U, Mohn E, Schäffel F, Schultz L, Rellinghaus B, Blüher A and Mertig M 2007 Regular arrangement of nanoparticles from the gas phase on bacterial surface-protein layers *Appl. Phys. Lett.* **90** 113114

[29] Howland M, Szmodis A, Sanii B and Parikh A 2007 Characterization of physical properties of supported phospholipid membranes using imaging ellipsometry at optical wavelengths *Biophys. J.* **92** 1306–17

[30] Erbe A and Sigel R 2007 Tilt angle of lipid acyl chains in unilamellar vesicles determined by ellipsometric light scattering *Eur. Phys. J.* E **22** 303–9

[31] Wagner R S and Ellis W C 1964 Vapor–liquid–solid mechanism of single crystal growth *Appl. Phys. Lett.* **4** 89–90

[32] Richter R P, Bérat R and Brisson A R 2006 Formation of solid-supported lipid bilayers: an integrated view *Langmuir* **22** 3497–505

[33] Wu Z, Xiang H, Kim T, Chun M-S and Lee K 2006 Surface properties of submicrometer silica spheres modified with aminopropyltriethoxysilane and phenyltriethoxysilane *J. Colloid Interface Sci.* **304** 119–24

[34] Wiegand G, Arribas-Layton N, Hillebrandt H, Sackmann E and Wagner P 2002 Electrical properties of supported lipid bilayer membranes *J. Phys. Chem.* B **106** 4245–54

[35] Soumpasis D M 1983 Theoretical analysis of fluorescence photobleaching recovery experiments *Biophys. J.* **41** 95–7

[36] Noy A, Artyukhin A B and Misra N 2009 Bionanoelectronics with 1d materials *Mater. Today* **12** 22–31

[37] Tang E and Dong S 2009 Preparation of styrene polymer/ZnO nanocomposite latex via miniemulsion polymerization and its antibacterial property *Colloid Polym. Sci.* **287** 1025–32

[38] Leonenko Z, Carnini A and Cramb D 2000 Supported planar bilayer formation by vesicle fusion: the interaction of phospholipid vesicles with surfaces and the effect of gramicidin on bilayer properties using atomic force microscopy *Biochim. Biophys. Acta* **1509** 131–47

[39] Huang Y, Palkar P V, Li L-J, Zhang H and Chen P 2010 Integrating carbon nanotubes and lipid bilayer for biosensing. bioelectron *Biosens. Bioelectron.* **25** 1834–7

[40] Huang C and Mason J T 1978 Geometric packing constraints in egg phosphatidylcholine vesicles *Proc. Natl Acad. Sci. USA* **75** 308–10

[41] Dayani Y and Malmstadt N 2012 Lipid bilayers covalently anchored to carbon nanotubes *Langmuir* **28** 8174–82

[42] Moura S P and Carmona-Ribeiro A M 2005 Biomimetic particles: optimization of phospholipid bilayer coverage on silica and colloid stabilization *Langmuir* **21** 10160–4